

F.M. Everaerts (Editor), *Analytical Isotachophoresis*
© 1981 Elsevier Scientific Publishing Company, Amsterdam -- Printed in The Netherlands

33

A NEW APPROACH TO AUTOMATED ISOTACHOPHORESIS WITH MULTICHANNEL ZONE DETECTION

ERNST SCHUMACHER, WOLFGANG THORMANN, and DIETER ARN

Institut für anorganische und physikalische Chemie der Universität Bern,
Freiestrasse 3, CH-3012 Bern

1. One of the early publications on isotachophoresis used a simple apparatus in which a filter paper strip in an insulating cooling bath served as carrier for the LE (leading electrolyte), SS (separand solution) and TE (terminating electrolyte) (ref. 1). The component zones were detected simultaneously e.g. by reagent sprays or autoradiography (labelled separands). Since no buffer was added, zone boundaries were also revealed by a scan with a tiny glass-electrode along the wet strip. Konstantinov et al. (ref. 2) proposed a version of simultaneous detection of all zone boundaries in a quartz capillary. They observed a diffraction pattern which changed with the refractive index of the zones of e.g. chloro-complexes of heavy metals. Hjertén et al. (ref. 3) scanned a quartz-tube repeatedly at two UV-frequencies and obtained information on the time-development of the isotachophoretic pattern with AMP, ADP, and ATP. Hinckley (ref. 4) mentions isotachophoresis as an automatable method of analysis for electrolytes.

2. We were led to investigate automated isotachophoresis with multichannel detection (ref. 5) in order to shorten the duration of an analysis, to gain information on the validity of the Kohlrausch steady state condition, and to increase the precision of the zone lengths by multiple independent measurements.

Where applicable, isotachophoresis produces simple rectangular concentration distributions of separands (if the finite width of the boundaries between components is neglected). Because this is a moving pattern, each zone exhibits a characteristic field strength ($E = |\vec{E}|$) which changes abruptly between zones. In weakly buffered systems there is a stepwise monotonous increase of E from the LE through the pattern to the diffuse boundary of the TE and the sample origin (inversions (ref. 6) are very rare indeed in contrast to strongly buffered systems; where they are common (ref. 7)). It is, therefore, not necessary to wait at the end of the separation device in order to detect the zones as it is mandatory e.g. in HPLC or GC, where highly non linear adsorption isotherms require a comparable number of HETP's for each separand for evaluation.

Best Available Copy

The material on this page was copied from the collection of the National Library of Medicine by a third party and may be protected by U.S. Copyright law.

34

Since the field strength is the most general physical property characterizing the separand pattern, its quasi-continuous measurement at many points along the column gives the necessary information about

- the evolution of mixed zones into separate zones, Fig. 1 and Fig. 4,
- the approach to the steady state pattern for every boundary and, therefore, the minimum time for a valid isotachophoretic measurement of each zone length.

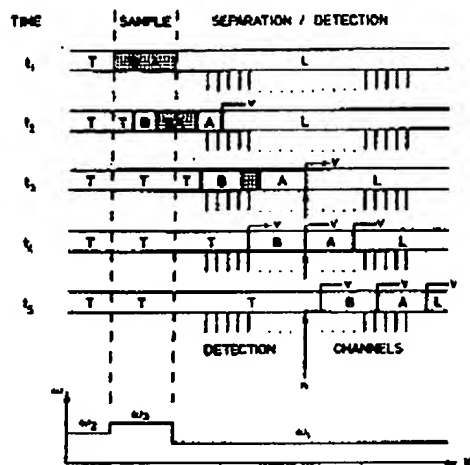


Fig. 1. Schematic of a two-component isotachophoretic separation with multiple detection channels. At bottom: Kohlrausch's Omega function. For a practical example refer to Fig. 4.

3. We use an equidistant array of 255 electrode pairs perpendicular to the column (electrodes 50 μm wide, 500 μm thick, distance of the pairs 340 μm) which reside on a thin glass plate. This forms one wall of the rectangular separation column (dimensions 1 \times 0.2 mm^2); a plastic gasket defines the channel which is closed by a methacrylate slab. The glass-electrode carrier is in good thermal contact with a water- or Peltier-cooled aluminum slab. In Fig. 2 a schematic of the multichannel detection system together with the auxiliary devices is shown. The handling of the fluids is accomplished through appropriate channels in and stop-cocks attached to the methacrylate body. In Fig. 3 the electrode array is

reproduced. It is not possible to resolve the fine electrodes along the column without glossy print. The electric field strength scan takes place over the wide enlarged end of the electrodes. It consists of a pair of graphite points (medium hard pencils) which are moved from pair to next pair by a stepper motor. In Fig. 4 a two component mixture is measured at five different electrode pairs, used as single detectors. Fig. 5 exhibits the field strength scan at channel 220 of a 14 component analysis for comparison with conventional methodology.

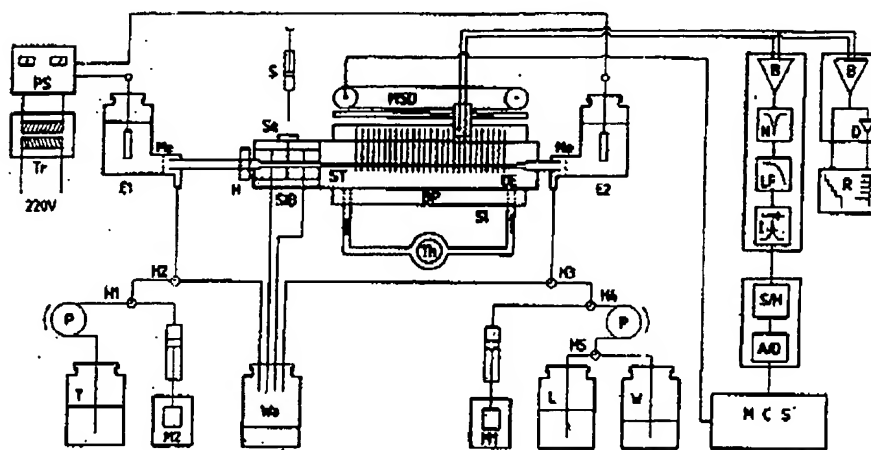


Fig. 2. Schematic of the multichannel isotachophoretic unit.

A/D analog to digital converter; B buffer; BP block of plastics; D differentiator; DE detection electrodes; E1 Pt-electrode vessel with terminating electrolyte; E2 Pt-electrode vessel with leading electrolyte; H screw for opening and closing of SIB; H1-5 3-way stopcock with 90° channel; I isolation amplifier; LF low pass filter; M1 piston pump for counterflow; M2 piston pump for pushing; MCS microcomputersystem with H8-computer, floppy disk, CRT terminal, printer; Me membranes; MSD mechanical scanning device; N notch filter; P peristaltic pump; PS constant current power supply; R two channel recorder; S sample syringe; Se septum; S/H sample and hold; SIB sample inlet block; S1 slab; ST separation and detection tube; T terminating electrolyte; Th thermostat; Tr 220V/24V transformer with separated primary/secondary and isolation for >20 kV; W water; Wa waste.

36

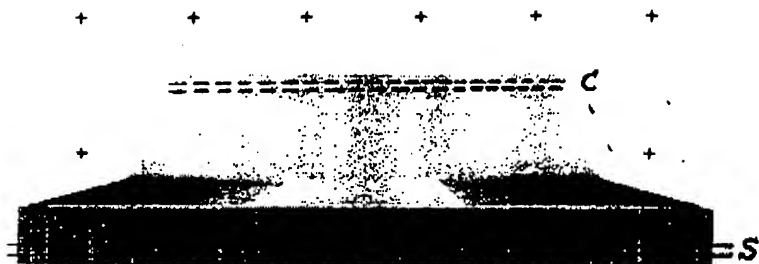


Fig. 3. Array of 256 Electrodes on a glass plate. C marks the separation column. S the scan path.

4. Automation of isotachophoresis and evaluation of the measurements is accomplished in this set-up with the following means. One measurement takes \approx 30 msec. The digital readout at every pair is successively stored in the RAM of a microprocessor system. After a controlled scan of the 255 pairs the data is analyzed with the following algorithms:

- rough identification of the boundaries by $\Delta E/\Delta x$ spikes,
- integration of the $E(x)$ curve (summation at equidistant points),
- straight line fit by least squares for each zone,
- interpolation of precise zone boundaries at the intersection of two neighbouring straight lines,
- storing zone boundaries.

These operations take place during the backtrace of the scan-electrodes (approx. 1 sec). Between successive scans the speed of the boundaries is obtained. As soon as this is equal for every boundary and spurious boundaries have vanished, the microprocessor takes 10 zone length measurements and determines their means and standard deviations. A resolution of $\pm 50 \mu\text{m}$ is easily obtained. Finally the lengths are corrected for the time lag between the measurements at different electrode pairs. The analytical results are in digital form together with a standard error. If a calibration matrix of appropriate mobility data is stored, mole numbers or any other representation of absolute or relative composition can be printed. Calibration is automated with a special component mixture appropriate to the sample series under test.

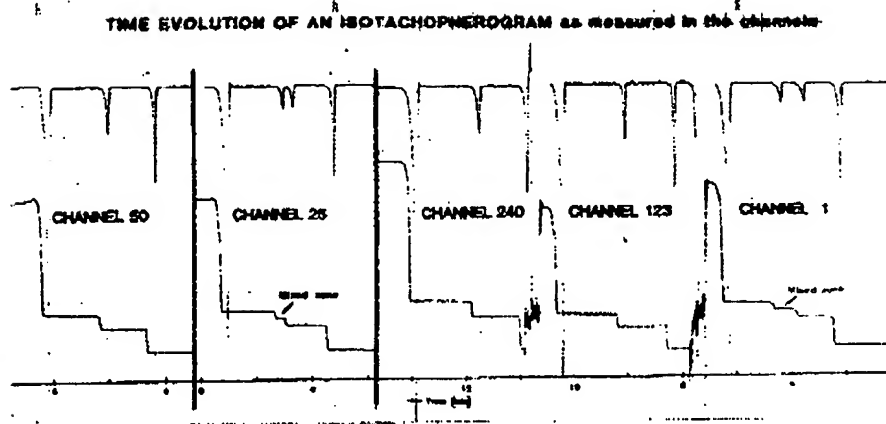


Fig. 4. Two-component mixture measured at five different channels illustrating the schematic of Fig. 1.

Leading electrolyte	hydrochloric acid 2.5×10^{-3} M
Terminating electrolyte	sodium lactate 10^{-2} M
Counter ion	H_3O^+
Solvent	water
Additive to leading electrolyte	0.05 % Mowiol
Separation tube	width 1 mm height 0.4 mm length 19.6 cm
Electrodes	width 0.06 mm interval 0.34 mm number 256
Injected sample volume	12 μl
Sample solution	maleic acid 1.22×10^{-3} M phosphoric acid 1.26×10^{-3} M
Migration current	200 μA
Separation time	~ 7 min

38

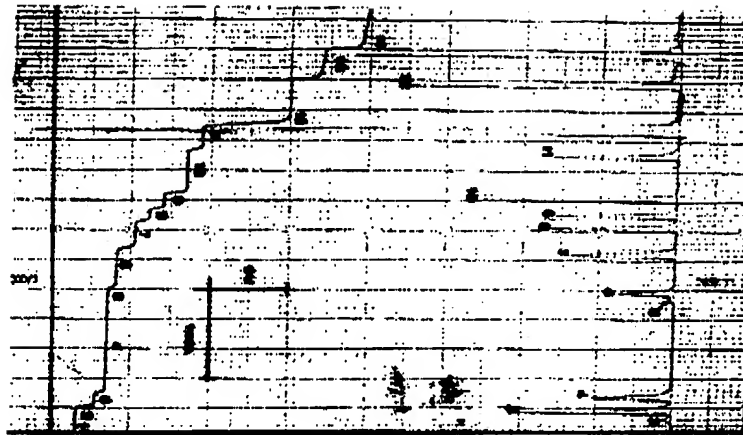


Fig. 5. 14-component analysis at channel 220. Above differentiated signal.

Leading electrolyte	hydrochloric acid 2.5×10^{-3} M
Terminating electrolyte	sodium acetate 10^{-2} M
Counter ion	H_3O^+
Solvent	water
Additive to leading electrolyte	0.05 % Mowiol
Injected sample volume	12 μl
Migration current	150 μA
Detection after separation in channel	220
Separation time	~ 10 min

	pK _a	pH
1 Hydrochloric acid	-6	2.60
2 Nitric acid	-1.32	2.62
3 Maleic acid	1.83	2.94
4 Phosphoric acid	2.12	2.99
5 Nitrous acid	3.20	3.02
6 Chloracetic acid	2.85	3.02
7 Tartaric acid	2.98	3.02
8 Citric acid	3.14	3.06
9 Malic acid	3.40	3.14
10 Glycolic acid	3.831	3.35
11 Lactic acid	3.868	3.38
12 Ascorbic acid	4.10	3.53
13 Glutamic acid	4.20	3.72
14 Acetic acid	4.76	3.82

} Inversion!
} $\Delta pK = 0.027$:

5. The advantages of this multichannel detection over conventional single detectors are manyfold:

- information about the time-evolution of the separation pattern is secured. This very often contributes to the identification of zones. It enables kinetic measurements in systems with chemical reaction boundaries (ref. 8);
- a quantitative criterion for the validity of the isotachophoretic state for every zone boundary is obtained (constant speed, constant zone length within predetermined and controlled error-bounds);
- simultaneous measurement of all zone boundaries leads automatically to the mi-
- the measuring and evaluation processes are completely automatic;
- the microprocessor, its auxiliary chips and output devices with programs in EPROM costs less than a strip chart recorder. It is easily possible to add a visible analog readout of the zone pattern in order to directly observe the evolution of the analysis.

We have not yet attached an automatic sampling system because this part of the process has been solved with other analytical methods. It is feasible to realize the same advantages with other detectors, e.g. using differences of refractive index or UV-absorption with appropriate scanning devices under microprocessor-control.

ACKNOWLEDGEMENTS

We should like to thank CIBA-GEIGY AG for financial support of this work. This project is sponsored by the "Kommission zur Förderung der wissenschaftlichen Forschung", Grant No. 1074.

REFERENCES

- 1 E. Schumacher & T. Studer, Helv.chim.acta 47 (1964) 957.
The apparatus was described in W. Friedli & E. Schumacher, Helv.chim.acta 44 (1961) 1829 and the theory in E. Schumacher, University of California, Lawrence Radiation Laboratory publication UCRL-10624, 1963, p. 210.
- 2 B.P. Konstantinov & O.V. Oshurkova, Dokl.Akad.Nauk SSSR 148 (1963) 1110.
- 3 S. Hjertén, Protides Biol.Fluids, Proc.Colloq. 22 (1975) 669; S. Hjertén, L.G. Överstedt & G.J. Johansson, J.Chromatography 194 (1980) 1.
- 4 J.O.N. Hinckley, Clin.Chem. 20 (1974) 973.
- 5 E. Schumacher, P. Ryser & W. Thormann, Helv.chim.acta 60 (1977) 3012.
- 6 see ref. 1, E. Schumacher & T. Studer, loc.cit.
- 7 F.E.P. Mikkers & F.M. Everaerts, this symposium.
- 8 E. Schumacher, Helv.chim.acta 40 (1957) 2322.

**This Page is Inserted by IFW Indexing and Scanning
Operations and is not part of the Official Record**

BEST AVAILABLE IMAGES

Defective images within this document are accurate representations of the original documents submitted by the applicant.

Defects in the images include but are not limited to the items checked:

- BLACK BORDERS**
- IMAGE CUT OFF AT TOP, BOTTOM OR SIDES**
- FADED TEXT OR DRAWING**
- BLURRED OR ILLEGIBLE TEXT OR DRAWING**
- SKEWED/SLANTED IMAGES**
- COLOR OR BLACK AND WHITE PHOTOGRAPHS**
- GRAY SCALE DOCUMENTS**
- LINES OR MARKS ON ORIGINAL DOCUMENT**
- REFERENCE(S) OR EXHIBIT(S) SUBMITTED ARE POOR QUALITY**
- OTHER:** _____

IMAGES ARE BEST AVAILABLE COPY.

As rescanning these documents will not correct the image problems checked, please do not report these problems to the IFW Image Problem Mailbox.